to be important in small organic molecules run as microcrystalline powders. In the atypical case of a simple compound exhibiting a very short $T_{1\rho}(H)$ value [e.g., anthracene[18] and 3,5-bis[(methylamino)carbonyl]-1-methyl-1,4-dihydropyridine[21]] and significantly different T_{CH} values, the signal intensities do not agree with atomic ratios. When polarization is incomplete, the equilibrium or steady-state condition in the thermodynamic model using a common spin temperature begins to break down, and quantitative results are not obtained.

Acknowledgment. This work was sponsored by the Division of Chemical Sciences, Office of Basic Energy Sciences of the Department of Energy, under Grant DE-AC02-78ER05006.

Registry No. 1, 596-31-6; **2**, 691-64-5; **3**, 886-38-4; **4**, 4741-53-1; **5**, 89-32-7.

Supplementary Material Available: Absolute intensity of the signals for **2** as a function of contact time (Table VIII) (1 page). Ordering information is given on any current masthead page.

Metal–Nitroxyl Interactions. 30. Single-Crystal EPR Spectra of Two Spin-Labeled Copper Porphyrins

Reddy Damoder, Kundalika M. More, Gareth R. Eaton,* and Sandra S. Eaton

Contribution from the Departments of Chemistry, University of Denver, Denver, Colorado 80208, and University of Colorado at Denver, Denver, Colorado 80202. *Received September 29, 1982*

Abstract: Rotated single-crystal EPR spectra have been obtained for two spin-labeled copper porphyrins doped into zinc tetraphenylporphyrin. Four conformations of the spin-label linkage were observed in each of the crystals. Analysis of the rotation dependence of the spin–spin splittings gave the isotropic exchange and anisotropic dipolar contributions to the spin–spin interaction. Values of the exchange coupling constant, J, ranged from -30 to $+10 \times 10^{-4}$ cm^{-1}. The interspin distance, r, ranged from 9.2 to 15.5 Å. There was no correlation between the values of r and J.

Introduction

Nitroxyl spin labels that are used to study biological systems sometimes are observed to interact with paramagnetic metals or other radicals.[1,2] The second paramagnetic center may be intrinsic to the system or purposely added as a second probe. The interpretation of the frozen solution EPR spectra of such systems involves separately estimating the exchange and dipolar contributions to the spin–spin interaction. Many interpretations in the literature assume that the exchange contribution is negligible so that spectra can be interpreted in terms of purely dipolar interaction from which metrical information can be directly obtained. Recent results from these laboratories have demonstrated that exchange interactions are significant at longer distances than previously were believed possible.[3,4] In many cases the exchange interaction, J, results in high resolution "AB" patterns in the fluid solution EPR spectra due to electron spin–electron spin coupling. The same splitting presists, albeit with different effects on line shapes, in frozen solution EPR spectra. We have shown that when dipolar and exchange contributions to the spin–spin interaction are of similar magnitude, the magnitude of each and the sign of J can be obtained by analysis of frozen solution EPR spectra.[5] In some of the frozen solution spectra studied in this initial attempt the lack of spectral resolution due to overlapping lines made the derived parameters (J, distance) uncertain.[5] It is clear that development of a sense of which features in the frozen solution EPR spectra are the best measures of the exchange and dipolar contributions requires some calibration experiments with single-crystal spectra. The analysis of the single-crystal spectra also provides a more stringent test of the computational approach to the spin–spin interaction than the powder spectra do. In addition, the single-crystal spectra provide a definitive separation of the exchange and dipolar contributions to the spin–spin interaction.

We have therefore examined the single-crystal EPR spectra of two spin-labeled copper porphyrins, I and II, doped into zinc

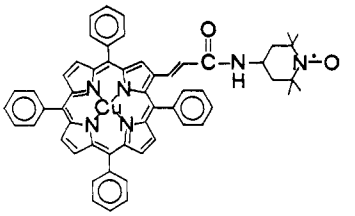

trans I
cis II

tetraphenylporphyrin. These complexes have previously been studied in fluid solution[3,6] and in frozen solution,[5] so the results of this study provide a comparison of the information which can be obtained in fluid solution, frozen solution, and single-crystal studies.

This study is the first complete analysis of the exchange and dipolar contributions to weak spin–spin interaction between nonequivalent unpaired electrons by single-crystal EPR spectroscopy.

Experimental Section

The compounds studied here were prepared by literature methods: I, II,[6] tetraphenylporphyrin,[7,8] zinc tetraphenylporphyrin (ZnTPP).[9] The visible spectrum of ZnTPP in benzene solution had bands at 589, 550, and 425 nm with log ϵ = 3.72, 4.45, and 5.85, respectively. The band positions agreed well with the literature values[10] and the extinction coefficients were greater than the literature values.[10] No EPR signal was

* Address correspondence to this author at the University of Denver.

(1) Berliner, L. J., Ed. "Spin Labeling II"; Academic Press: New York, 1979.
(2) Eaton, S. S.; Eaton, G. R. *Coord. Chem. Rev.* **1978**, *26*, 207–262.
(3) More, K. M.; Eaton, G. R.; Eaton, S. S. *Can. J. Chem.* **1982**, *60*, 1392–1401, and references therein.
(4) More, J. K.; More, K. M.; Eaton, G. R.; Eaton, S. S. *Inorg. Chem.* **1982**, *21*, 2455–2460, and references therein.
(5) Eaton, S. S.; More, K. M.; Sawant, B. M.; Boymel, P. M.; Eaton, G. R. *J. Magn. Reson.*, in press.
(6) More, K. M.; Eaton, S. S.; Eaton, G. R. *Inorg. Chem.* **1981**, *20*, 2641–2647.
(7) Adler, A. D.; Longo, F. R.; Finarelli, J. D.; Goldmacher, J.; Assour, J.; Korsakoff, L. *J. Org. Chem.* **1967**, *32*, 476.
(8) Rousseau, K.; Dolphin, D. *Tetrahedron Lett.* **1974**, 4251–4254.
(9) Adler, A. D.; Longo, F. R.; Kampas, F.; Kim, J. *J. Inorg. Nucl. Chem.* **1970**, *32*, 2443–2444.
(10) Dorough, G. D.; Miller, J. R.; Huennekens, F. M. *J. Am. Chem. Soc.* **1951**, *73*, 4315–4320.

0002-7863/83/1505-2147$01.50/0

observed for ZnTPP as a powder or a single crystal. Tetrahydrofuran (THF) was purified by distillation and stored under nitrogen in the dark. EPR spectra were obtained at room temperature on a Varian E-9 spectrometer. Data were collected digitally using a Varian 620-L103 minicomputer and the CLASS language. To improve the signal-to-noise ratio of the spectra, modulation amplitudes up to one-half the peak-to-peak line width were used to obtain the spectra. Although the use of such large modulation amplitudes causes slight distortion of the line shape, it should have no impact on the transition energies and negligible impact on the analysis of the spectra.

Single crystals were grown by slow evaporation (3 to 4 days) of a solution containing a 99:1 ratio by weight of ZnTPP:I or II in purified THF. Repeated recrystallization of the ZnTPP doped with I or II was necessary to obtain suitable crystals. The crystals used to obtain the EPR spectra were approximately 3 × 2 × 1.5 mm.

The crystals were mounted with silicone stopcock grease in a 3.5-mm segment of Wilmad synthetic quartz square cross section tubing (WQS-102, 2 mm i.d., 0.75 mm wall). A face of the holder was attached to the rod of a Varian E-229 one-cycle goniometer. The orientation of the crystal in the holder was adjusted iteratively to align the z axis of the copper A tensor with the rotation axis of the goniometer. Alignment was adjusted until rotation through 180° caused little change in the copper hyperfine splitting. Subsequent simulation of the spectra indicated that the z axis had been located within about 10°. The error in the z-axis orientation was taken into account in the simulations. EPR spectra were then collected at 15° intervals in this plane (xy plane). Similar arbitrary definitions of the x and y axes relative to the faces of the crystal were used for the crystals containing I and II. The goniometer was then attached successively to two perpendicular faces of the holder, and data were collected as in the first plane. The accuracy of the rotation angles was indicated by the fact that in each plane spectra taken at 180° agreed with those at 0 ± 1°.

Computer Simulations

The perturbation calculation used in the simulation of the spectra is similar to that described previously for the analysis of powder spectra of spin-labeled copper complexes.[5] The Hamiltonian (eq 1) consists of terms for independent electrons 1 (copper) and 2 (nitroxyl) as given in eq 2 and an interaction term as given in eq 3. The interaction term includes an isotropic exchange

$$\mathcal{H} = \mathcal{H}_1 + \mathcal{H}_2 + \mathcal{H}_{\text{int}} \quad (1)$$

$$\mathcal{H}_i = \sum_{j=x_i,y_i,z_i} (\beta g_j S_{ij} H_j + A_j S_{ij} I_{ij}) \qquad (i = 1, 2) \quad (2)$$

$$\mathcal{H}_{\text{int}} = -JS_1S_2 + \mathcal{H}_{\text{dipolar}} \quad (3)$$

interaction and an anisotropic dipolar interaction. The symbols in eq 1–3 have their usual meanings and are discussed in detail in ref 5 and 13. The splitting between the singlet and triplet levels is J and a negative sign of J indicates an antiferromagnetic interaction. The angles which define the relative orientations of the axes of electrons 1 and 2, the dipolar tensor, and the magnetic field direction are shown in Figure 1.

Two computer programs, using the same computational approach, were used to analyze the EPR spectra. ROTAN calculates the nitroxyl nitrogen hyperfine splitting and the spin–spin splitting of the nitroxyl $m_I = 0$ line as a function of rotation angle in three orthogonal planes and outputs plots of the splittings in gauss on a ZETA 1553 digital plotter. These plots were used to simulate graphs of the experimentally determined splittings as a functic · of orientation.

CRYST calculates the complete single crystal EPR line shape for a particular orientation of the crystal in the magnetic field and produces graphical output on a Calcomp plotter. The spectra of multiple species can be summed in a single simulation. Both copper isotopes and coupling of the copper electron to four equivalent nitrogens were included in the simulations. In the derivation of the equations used in the program it was assumed that for each electron the g and A tensors were collinear. The experimental data were consistent with this assumption within the accuracy of the data.

Analysis of EPR Spectra

Weak spin–spin interaction is expected to consist of an isotropic exchange interaction and an anisotropic dipolar interaction. The resulting EPR spectra have been referred to as AB patterns[2,11-13]

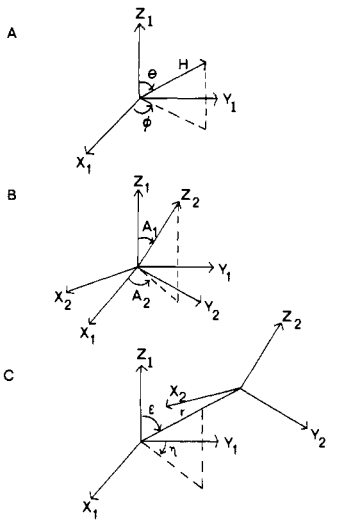

Figure 1. Definitions of angles and interspin vector. (a) The angles θ and ϕ define the orientation of the magnetic field relative to the axes of electron 1 (copper). (b) The angles A_1 and A_2 define the orientation of the z axis of electron 2 (nitroxyl) relative to the axes of electron 1 (copper). (c) The angles ϵ and η define the orientation of the interspin vector r relative to the axes of electron 1 (copper). Throughout the text r is used to denote the magnitude of the interspin vector.

by analogy with high-resolution NMR.[14] The interaction results in the splitting of each of the hyperfine lines for both of the electrons into doublets. To first approximation, when J is small, six nitroxyl lines and 144 copper lines are expected in the EPR spectrum of a spin-labeled copper porphyrin with resolved nitrogen hyperfine splitting on the copper lines. The 144 copper lines include the splittings due to the copper nuclear spin, two copper isotopes, nitrogen nuclear spins, and the spin–spin interaction. It is assumed that only $\Delta m_I = 0$ transitions are observed. There are actually 432 copper lines and 432 nitroxyl lines, but the splitting of the nitroxyl lines by the copper nuclear spin and by the spins of the nitrogens coordinated to the copper is less than the line widths of the nitroxyl lines. Similarly, the splitting of the copper lines by the nitroxyl nitrogen spin is too small to be resolved. Clearly the six nitroxyl lines are easier to analyze by inspection than the 144 copper lines. Thus the initial estimates of the spin–spin splittings discussed below were obtained from the nitroxyl lines. The simulations of the complete spectra indicated that the information obtained from the nitroxyl lines was in good agreement with the splittings observed for the copper lines.

Inspection of the nitroxyl region of the EPR spectra of either I or II in ZnTPP indicated up to 16 resolved lines at some orientations of the crystal. Thus it was clear that there was more than one AB pattern. The copper lines indicated that the orientation of the z axis of the copper hyperfine tensor was the same for all components of the spectrum. Comparison of the spectra in the three orthogonal planes indicated that the components did not arise from different orientations of the same species related by rotation around the copper z axis or reflection in the copper xy plane. Thus it was necessary to treat the spectra as the sum of contributions from species with different orientations and different spin–spin interaction parameters.

The magnetic field positions for the resolved lines in the spectra were plotted as a function of the orientation of the crystal. The lines were then grouped into nitrogen hyperfine triplets based on the criteria that the nitrogen hyperfine splitting must vary smoothly with orientation, that trends in A_N must correlate with trends in

(11) Schepler, K. L.; Dunham, W. R.; Sands, R. H.; Fee, J. A., Peles, R. H. *Biochim. Biophys. Acta* **1975**, *397*, 510–518.
(12) Buettner, G. R.; Coffman, R. E. *Biochim. Biophys. Acta* **1977**, *480*, 495–505.
(13) Boas, J. F.; Hicks, P. R.; Pilbrow, J. R.; Smith, T. D. *J. Chem. Soc., Faraday Trans. 2*, **1978**, *74*, 417–431.
(14) Abraham, R. J. "The Analysis of High Resolution NMR Spectra", Chapter 3, Elsevier: Amsterdam, 1971.

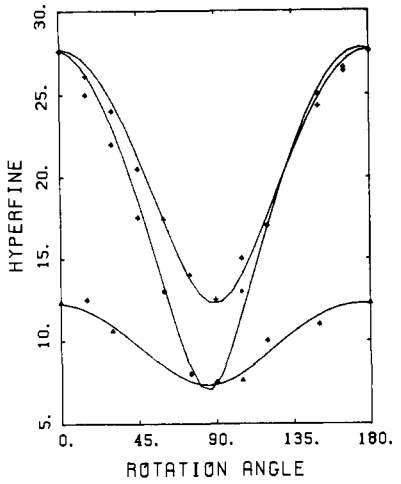

Figure 2. Plots of the orientation dependence of the nitroxyl nitrogen hyperfine splitting in gauss in three orthogonal planes for species 1–3 of spin-labeled copper complex I doped into ZnTPP. The experimental data are denoted by (▲), *xy* plane, (+), *xz* plane; (♦), *yz* plane. The solid lines are the calculated curves obtained with the parameters given in Tables I and II.

g value, and that the assignments at the intersections of the planes had to agree. The triplets were assigned to AB patterns using the criteria that the spin–spin splitting must vary smoothly with orientation, that the splitting could go through zero twice, at most, in the course of 180°, and that the AB patterns in the three planes had to match up at the intersections of the planes. For both I and II, these criteria could be met only by assigning the lines in the nitroxyl region of the spectrum to four species. The four species are discussed below. A few weak lines at some orientations of the crystals were not assigned. It is likely that there are other species present in the crystal with low populations or with greater line widths than those for which the analysis has been done. The lines in these cases would be difficult to detect.

For trans isomer I, species 2 gave the prominent nitroxyl lines at most orientations of the crystal. Species 1 gave well-resolved lines in the *yz* plane and at some orientations in the *xy* plane. Species 3 was present in lower abundance than the other species but gave well-resolved lines at some orientations in all three planes and the simulations of the spectra clearly confirmed its presence. Species 4 had broader lines than the other components of the spectra. Its parameters were well-defined only at orientations where the combined nitrogen hyperfine and spin–spin splittings for species 4 were larger than the splittings for the other species, with the result that the nitroxyl lines for species 4 came at higher and lower fields than the signals from the other species. In some cases it was possible only to detect the highest and lowest field lines for species 4. However, since the largest nitrogen hyperfine occurs when the magnetic field is along the *z* axis of the nitroxyl tensor, and the nitroxyl hyperfine splitting for species 4 was observable near this orientation, it was possible to define accurately the location of the nitroxyl *z* axis. Subtraction of twice A_N from the total splitting between the lowest and highest field lines at other orientations gave the spin–spin splitting.

For cis isomer II species 2 had the prominent lines at most orientations of the crystal. Species 1, 3, and 4 had lower populations than species 2 but gave well-resolved lines. At most orientations of the crystal two or more species gave overlapping lines, but the overall rotation dependence of the spectra permitted analysis of the separate components.

Approximate nitroxyl *g* and *A* values and orientations of the nitroxyl *g* and *A* tensors were obtained by diagonalization. Since there was some uncertainty in estimating the positions of the overlapping lines from the experimental spectra, the *g* and *A* values and orientations of the tensors were optimized by comparison of observed and calculated spectra at selected orientations of the crystals where the spectra were well-resolved. For trans isomer I, species 1, 2, and 3 appeared to have about the same *g* value and nitrogen hyperfine at all orientations of the crystal. Due to

Table I. Spin-Hamiltonian Parameters for Nitroxyl Electron[a]

cmpd	species	g_{xx}	g_{yy}	g_{zz}	A_{xx}	A_{yy}	A_{zz}
I	1, 2, 3	2.0095	2.0063	2.0025	6.5	11.5	26.0
I	4	2.0095	2.0063	2.0025	8.0	8.5	27.5
II	1–4	2.0083	2.0066	2.0030	8.0	9.0	28.5

[a] *A* values are in units of 10^{-4} cm^{-1}.

Table II. Orientation and Interaction Parameters[a]

cmpd	species	A_1	A_2	ϵ	η	r^b	J^c	population, %
I	1	173	85	77	−75	13.7	−21	26
I	2	175	85	82	−27	15.0	−12	35
I	3	173	85	68	10	13.0	1	4
I[d]	4	55	−35	85	45	15.5	−30	35
II	1	127	117	53	−55	10.8	7	22
II	2	127	117	63	−16	12.5	0	44
II	3	127	117	45	42	10.2	10	17
II	4	127	117	155	80	9.2	−4	17

[a] Parameters are defined in Figure 1. [b] *r* in angstroms. [c] *J* in units of 10^{-4} cm^{-1}. [d] The parameters for this species have greater uncertainties than the other species because the lines were resolved at only a few orientations.

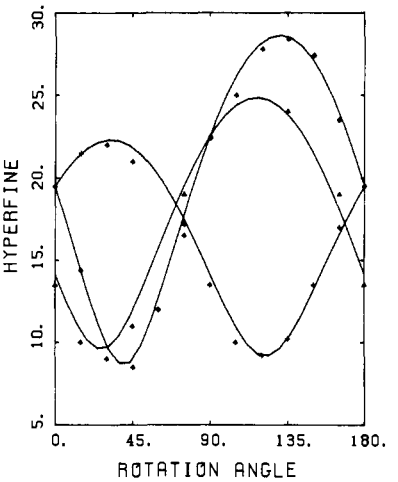

Figure 3. Plots of the orientation dependence of the nitroxyl nitrogen hyperfine splitting in gauss in three orthogonal planes for species 1–4 of spin-labeled copper complex II doped into ZnTPP. The experimental data are denoted by (▲), *xy* plane, (+), *xz* plane, (♦), *yz* plane. The solid lines are the calculated curves obtained with the parameters given in Tables I and II.

the overlap of the lines, there was an uncertainty of 2 to 3 G in the experimental values of the nitrogen hyperfine splittings at some orientations which could mask small differences in the *A* values and orientation of the hyperfine tensor for the individual species. At a few orientations of the crystal it was apparent that the hyperfine and *g* values were not identical for the three species, but the differences were too small to adequately define. Therefore it was assumed in the simulations that the nitroxyl hyperfine parameters were the same for species 1, 2, and 3. A plot of the orientation dependence of the hyperfine is given in Figure 2, the Hamiltonian parameters for the nitroxyl electron are given in Table I, and the angles defining the orientation of the nitroxyl tensors relative to the axes of the copper tensors are given in Table II. Since the nitroxyl *z* axis is less than 10° away from the copper *z* axis, the value of A_2 is highly uncertain. The nitroxyl hyperfine tensor for species 4 of trans isomer I was oriented differently than the nitroxyl hyperfine tensor in the other trans species (Table II). All four species of the cis isomer had similar orientations of the hyperfine tensor. Although the orientations were not identical, the differences were less than the experimental uncertainty at most orientations of the crystal. The orientation dependence of the hyperfine splitting is shown in Figure 3, the Hamiltonian parameters are given in Table I, and the angles defining the ori-

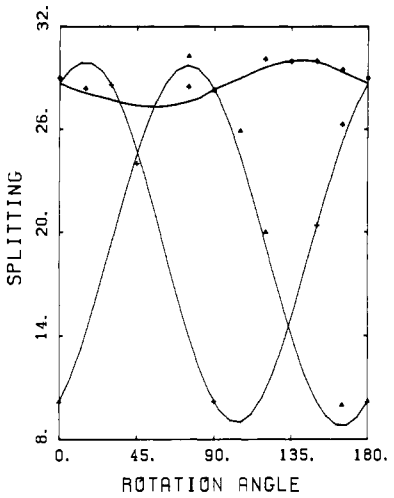

Figure 4. Plots of the orientation dependence of the spin–spin splitting in gauss in three orthogonal planes for species 1 of trans isomer I doped into ZnTPP. The experimental data are denoted by (▲), *xy* plane, (+), *xz* plane, (♦), *yz* plane. The solid lines are the calculated curves obtained with the parameters given in Table II.

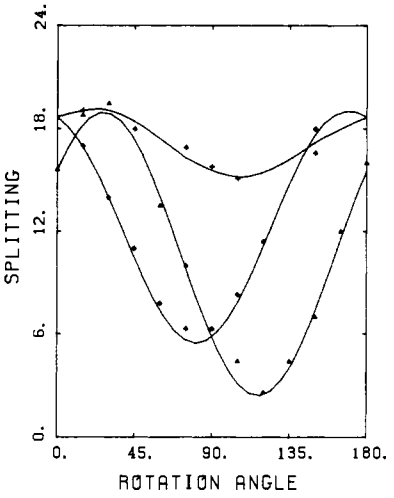

Figure 5. Plots of the orientation dependence of the spin–spin splitting in gauss in three orthogonal planes for species 2 of trans isomer I doped into ZnTPP. The experimental data are denoted by (▲), *xy* plane, (+), *xz* plane, (♦), *yz* plane. The solid lines are the calculated curves obtained with the parameters given in Table II.

entation of the nitroxyl *g* and *A* tensors are given in Table II. The *g* and *A* values shown in Table I for I and II are in good agreement with literature values for other piperidinyl nitroxyl radicals: tempone, g_{xx}, 2.0096; g_{yy}, 2.0063; g_{zz}, 2.0022; A_{xx}, 3.9; A_{yy}, 5.7; A_{zz}, 31.3 × 10^{-4} cm^{-1};[15] and for 4-piperidinyl maleimide, g_{xx}, 2.0087; g_{yy}, 2.0056; g_{zz}, 2.0022; A_{xx}, 7.6; A_{yy}, 7.0; A_{zz}, 33.0 × 10^{-4} cm^{-1}.[16]

The Hamiltonian parameters for the copper electron were obtained by computer simulation of the spectra and are given in Table III. The *g* values are in reasonable agreement with literature values for a single crystal of CuTPP in free base tetraphenylporphyrin: $g_{\parallel}$, 2.190; $g_{\perp}$, 2.045.[17] The literature values for the ^{63}Cu hyperfine coupling constant are $A_{\parallel}$, 201; $A_{\perp}$, 33 × 10^{-4} cm^{-1} in free tetraphenylporphyrin,[17] and $A_{\parallel}$, 205; $A_{\perp}$, 34 × 10^{-4} cm^{-1} in ZnTPP(H_2O).[18] The values of both $A_{\parallel}$ and $A_{\perp}$

Table III. Spin-Hamiltonian Parameters for Copper Electron[a]

cmpd	g_{xx}	g_{yy}	g_{zz}	A_{xx}^{Cu}	A_{yy}^{Cu}	A_{zz}^{Cu}	A_{xx}^{N}	A_{yy}^{N}	A_{zz}^{N}
I	2.049	2.045	2.202	24.0	23.0	194.0	14.4	14.4	17.6
II	2.047	2.049	2.200	24.0	23.5	192.0	14.6	14.6	17.6

[a] *A* values are in units of 10^{-4} cm^{-1}.

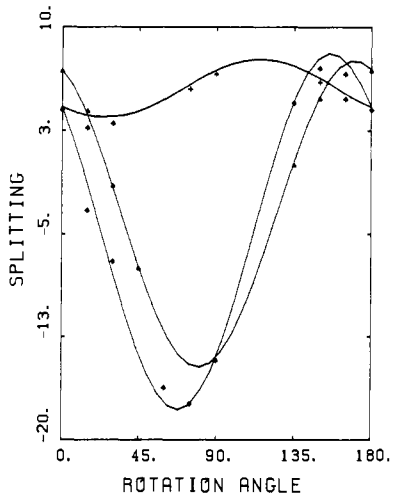

Figure 6. Plots of the orientation dependence of the spin–spin splitting in gauss in three orthogonal planes for species 3 of trans isomer I doped into ZnTPP. The experimental data are denoted by (▲), *xy* plane, (+), *xz* plane, (♦), *yz* plane. The solid lines are the calculated curves obtained with the parameters given in Table II.

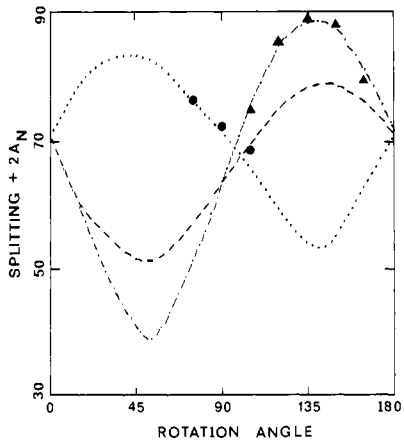

Figure 7. Plots of the sum of the spin–spin splitting plus twice the nitroxyl nitrogen hyperfine splitting in gauss in three orthogonal planes for species 4 of trans isomer I doped into ZnTPP. The experimental data are denoted by (▲), *xy* plane; (●), *xz* plane; (♦), *yz* plane. The calculated curves obtained with the parameters given in Tables I and II are denoted by (–), *xy* plane, (···), *xz* plane, (– –) *yz* plane.

obtained in this study are smaller than the values reported in the literature, which may reflect the effect of THF coordination to the copper. The values of $A_{\parallel}$ and $A_{\perp}$ obtained for CuTPP doped into ZnTPP and crystallized from THF solution were similar to the values obtained for I and II, so the differences from the literature values are not due to the spin-labeled substituent.

In the simulation of the copper spectra it was assumed that the four porphyrin nitrogens were equivalent. However, it has been noted that the *z* axis of the nitrogen hyperfine tensor falls along the N–Cu bond.[19] Therefore the nitrogens will not be equivalent except at special orientations of the molecule. The differences were too small to be resolved in these spectra. The actual *z* component of the nitrogen hyperfine tensor was obtained from the apparent splittings as reported by Guzy et al.[19] The values obtained for the nitrogen hyperfine components are in good

(15) Dalton, L. R.; Robinson, B. H.; Dalton, L. A.; Coffey, P. *Adv. Magn. Reson.* **1976**, *8*, 149–259.
(16) Beth, A. H.; Perkins, R. C., Jr.; Venkataramu, S. D.; Pearson, D. E.; Park, C. R.; Park, J. H.; Dalton, L. R. *Chem. Phys. Lett.* **1980**, *69*, 24–28.
(17) Manoharan, P. T.; Rogers, M. T. In "Electron Spin Resonance of Metal Complexes"; Yen, Y. F.; Ed.; Plenum Press: New York, 1969; pp 143–173.
(18) Brown, T. G.; Hoffman, B. M. *Mol. Phys.* **1980**, *39*, 1073–1109.
(19) Guzy, C. M.; Raynor, J. B.; Symons, M. C. R. *J. Chem. Soc. A* 1969, 2299–2303.

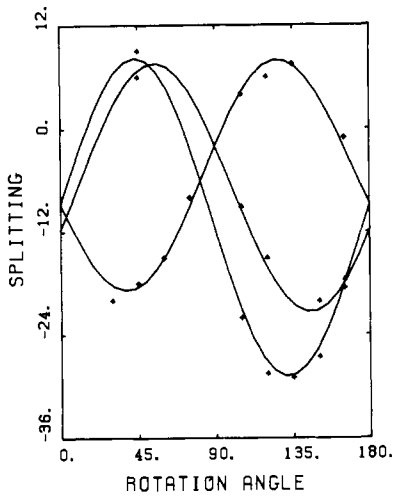

Figure 8. Plots of the orientation dependence of the spin–spin splitting in gauss in three orthogonal planes for species 1 of cis isomer II doped into ZnTPP. The experimental data are denoted by (▲), *xy* plane, (+), *xz* plane, (♦), *yz* plane. The solid lines are the calculated curves obtained with the parameters given in Table II.

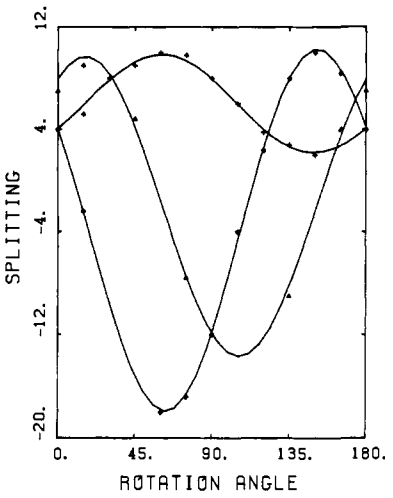

Figure 9. Plots of the orientation dependence of the spin–spin splitting in gauss in three orthogonal planes for species 2 of cis isomer II doped into ZnTPP. The experimental data are denoted by (▲), *xy* plane, (+), *xz* plane, (♦), *yz* plane. The solid lines are the calculated curves obtained with the parameters given in Table II.

agreement with the values obtained from ENDOR spectra: A^N_{xx}, 14.3; A^N_{yy}, 14.7; A^N_{zz}, 18.1 × 10^{-4} cm^{-1}.[18]

The observed spin–spin splittings for each of the species were plotted as a function of orientation. The plots were simulated using the program ROTAN to obtain values of r and J and the angles defining the orientation of the dipole interaction tensor. Plots of the experimental and calculated orientation dependence of the spin–spin splittings for species 1–3 of trans isomer I are given in Figures 4–6. Since the lowest and highest field lines of trans isomer I species 4 were resolved at some orientations of the crystal where the other lines from species 4 were not resolved, the data for this species were plotted as the sum of twice A_N plus the spin–spin splitting (Figure 7). The plots of the calculated and observed orientation dependence of the spin–spin splitting for species 1–4 of cis isomer II are given in Figures 8–11. The values of r, J, and the angles defining the orientation of the dipole interaction tensor that were obtained from simulation of the plots shown in Figures 4–11 were used as inputs to CRYST to simulate the complete line shapes. Spectra at most orientations were simulated with the approximate parameters to check that line positions in the simulations fell within 2 to 3 G of the observed lines. The parameters were then optimized to match the spectra at selected orientations which exhibited well-resolved lines. The final values of the orientation and interaction parameters are given in Table II. The uncertainties in the parameters are: angles, ±5°; r, ±0.5 Å; J, ±2 × 10^{-4} cm^{-1}.

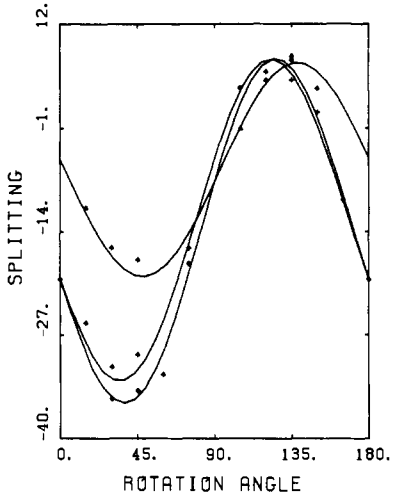

Figure 10. Plots of the orientation dependence of the spin–spin splitting in gauss in three orthogonal planes for species 3 of cis isomer II doped into ZnTPP. The experimental data are denoted by (▲), *xy* plane, (+), *xz* plane; (♦), *yz* plane. The solid lines are the calculated curves obtained with the parameters given in Table II.

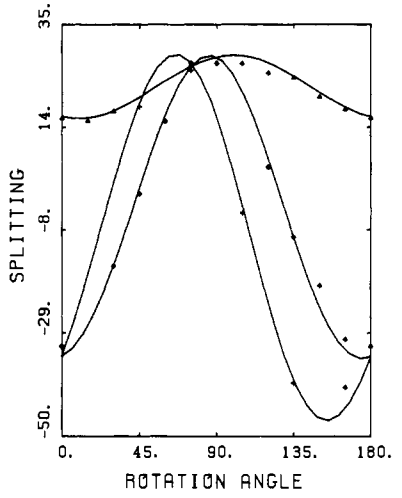

Figure 11. Plots of the orientation dependence of the spin–spin splitting in gauss in three orthogonal planes for species 4 of cis isomer II doped into ZnTPP. The experimental data are denoted by (▲), *xy* plane; (+), *xz* plane; (♦), *yz* plane. The solid lines are the calculated curves obtained with the parameters given in Table II.

The extensive overlap of the lines made it difficult to determine line widths accurately. However, it was observed that within a nitroxyl triplet the line widths were similar, but the line widths of the inner and outer lines of an AB pattern differed by about 2 to 5 G. Therefore in the simulations the same line width was used for the three lines of a nitrogen hyperfine triplet, but different widths were used for the inner and outer triplets of an AB pattern. The line widths for the nitroxyl lines were approximately 2.2 to 9 G and the copper line widths were about 4 to 16 G. Larger line widths were observed for species with larger values of J and/or smaller values of r. Because of the extensive overlap of the lines in the spectra, no attempt was made to exactly match the line widths in the simulated spectra with the experimental line widths. The copper $m_I = -3/2$ lines were found to be broader than the $m_I = \pm 1/2$ lines, although this difference was not incorporated into the simulations. The copper $m_I = 3/2$ lines were obscured by the nitroxyl lines. The broadening of the $m_I = -3/2$ lines may be due to g strain and/or A strain as discussed by Froncisz and Hyde.[20,21]

(20) Froncisz, W.; Hyde, J. S. *J. Chem. Phys.* **1980**, *73*, 3123–3131.

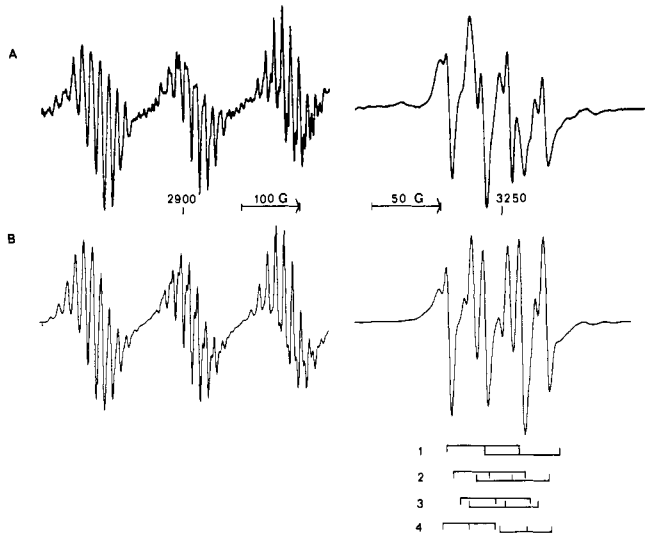

Figure 12. X-band (9.104 GHz) EPR spectra of trans isomer I doped into ZnTPP for $\theta = 30°$ and $\phi = -90°$. (A) The copper and nitroxyl regions of the experimental spectrum. There is a 16-G overlap of the high-field portion of the 520-G scan of the copper lines and the low-field portion of the 200-G scan of the nitroxyl lines. The spectra were obtained with 2 G modulation amplitude and 5 mW power. The gain used to record the copper lines was 12.5 times that used to record the nitroxyl lines. (B) Calculated spectra obtained for the parameters given in Tables I–III. The zero-crossing points for the nitroxyl hyperfine triplets for each of the species are shown schematically below the calculated spectrum.

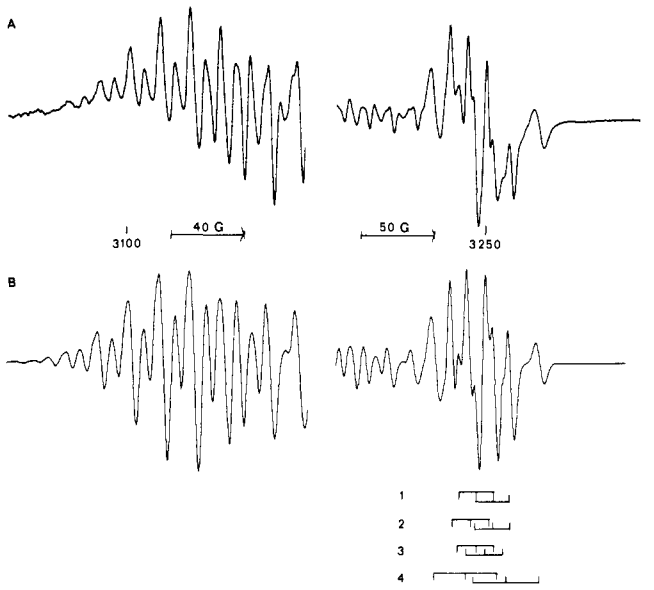

Figure 13. X-band (9.107 GHz) EPR spectra of trans isomer I doped into ZnTPP for $\theta = 90°$ and $\phi = 0°$. (A) The copper and nitroxyl regions of the experimental spectrum. There is a 57 G overlap of the high-field portion of the 165-G scan of the copper lines and the low-field portion of the 200-G scan of the nitroxyl lines. The spectra were obtained with 2 G modulation amplitude and 5 mW power. The gain used to record the copper lines was 10 times that used to record the nitroxyl lines. (B) Calculated spectra obtained for the parameters given in Tables I–III. The zero-crossing points for the nitroxyl hyperfine triplets for each of the species are shown schematically below the calculated spectrum.

Results and Discussion

When copper porphyrin I or II is doped into a single crystal, the spin-labeled side chain could be located at any of the eight pyrrole carbons and could be oriented above or below the porphyrin plane. Thus there are 16 possible locations for the side chain. Locations related by rotation around the copper z axis or reflection in the copper xy plane will give distinguishable spectra, but locations related by inversion will be indistinguishable at all orientations of the crystal. In the crystals of either I or II doped into ZnTPP, four distinct locations of the side chain were observed. The species with the side chain at the four different locations are identified as species 1–4, as sketched in III, and correspond to

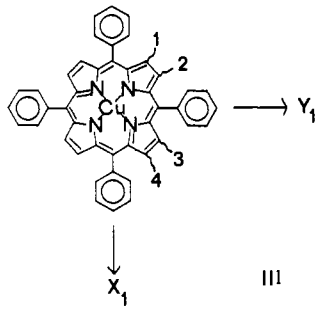

III

values of η of −75, −27, 10, and 45°, respectively, for the trans isomer and values of η of −55, −16, 42, and 80°, respectively for the cis isomer. Diagram III is drawn with the x and y axes along the phenyl rings. Since the orientation of the molecules in the crystal is not known, this is an arbitrary assignment. Also, since the g and A tensors for the copper electron are nearly axial, there is no molecular definition of the x and y axes. However, the 35 to 45° increments in the values of η indicate that species 1–4 differ because the spin-label substituent is located at four different pyrrole carbons independent of how the axes are defined. For both I and II it was found that the values of ϵ, r, and J were different for species 1–4. This is attributed to different conformations of the spin-labeled side chain in the four distinguishable species. The conformations may arise from crystal packing forces that are different at the four locations or from conformations of the molecule that are inherently similar in energy.

Figure 12 shows the spectrum of I obtained for $\theta = 30°$ and $\phi = -90°$. At this orientation the copper hyperfine splitting was 170 G and the nitroxyl nitrogen hyperfine splitting for species 1–3 was 26 G. In the nitroxyl region of the spectrum the signals from species 1–3 were partially resolved but the lines from species 4 were obscured by the sharper signals from species 1–3. The zero-crossing points for the nitroxyl triplets for each of the species are marked below the simulated spectrum. The separation between the centers of the two triplets for each species is the spin–spin splitting. Figure 13 shows the spectrum of I obtained for $\theta = 90°$ and $\phi = 0°$, i.e., when the magnetic field was along the copper x axis. At this orientation the copper hyperfine splitting was 25 G and the nitroxyl nitrogen hyperfine splitting for species 1–3 was 12 G. The nitroxyl lines from species 1 gave an apparent 4-line pattern with the spin–spin splitting approximately equal to the nitrogen hyperfine splitting. The spin–spin splittings for species 2 and 3 were smaller than the nitrogen hyperfine splitting. Thus the contributions from species 1–3 occurred within a small field range. The low-field and high-field nitroxyl signals from species 4 were well resolved from the signals for species 1–3. Part of the copper spectrum is shown at the same scale as the nitroxyl lines to show that the relative intensities of the lines are well-matched by the calculated spectra. When only one species was included in the simulations, not only were many of the experimental lines in the nitroxyl and copper portions of the spectrum not present, but the relative intensities of the copper and nitroxyl lines could not be matched.

The values of r for the four species observed for trans isomer I doped into ZnTPP were between 13.0 and 15.5 Å and the values of ϵ were between 68.5 and 85° (Table II). The values of r and ϵ are correlated, with larger values of r occurring for larger values of ϵ. This pattern is consistent with molecular models which indicated that as the nitroxyl ring was pushed toward the porphyrin plane (increasing value of ϵ), the value of r increased. The values of J for the four species ranged from −30 to +1 × 10^{-4} cm^{-1}. The variation in the values of J indicated that the exchange interaction was strongly dependent on the conformation of the spin–label linkage.

(21) Hyde, J. S.; Froncisz, W. *Ann. Rev. Biophys. Bioeng.* **1982**, *11*, 391–417.

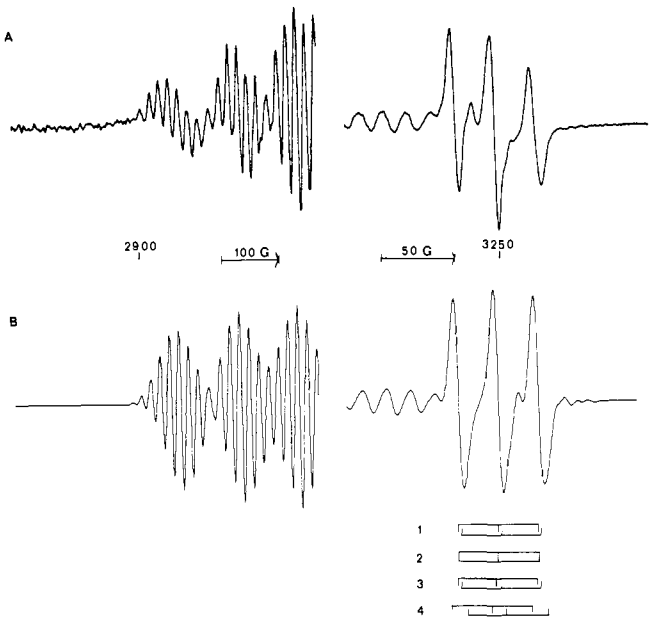

Figure 14. X-band (9.103 GHz) EPR spectra of cis isomer II doped into ZnTPP for $\theta = 117°$ and $\phi = 90°$. (A) The copper and nitroxyl regions of the experimental spectrum. There is a 65 G overlap of the high-field portion of the 520-G scan of the copper lines and the low-field portion of the 200-G scan of the nitroxyl lines. The spectra were obtained with 5 mW power and modulation amplitudes of 2 and 1.25 G for the copper and nitroxyl lines, respectively. The gain used to record the copper lines was 10 times that used to record the nitroxyl lines. (B) Calculated spectra obtained for the parameters given in Table I–III. The zero-crossing points for the nitroxyl hyperfine triplets for each of the species are shown schematically below the calculated spectrum.

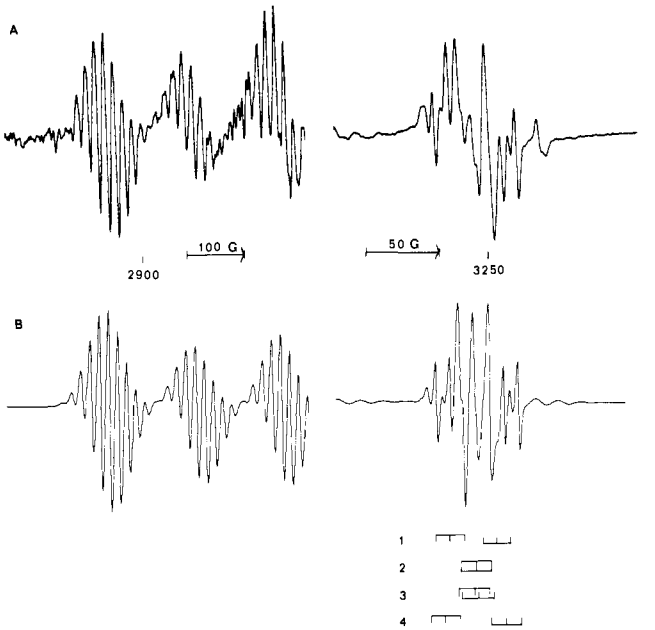

Figure 15. X-band (9.103 GHz) EPR spectra of cis isomer II doped into ZnTPP for $\theta = 135°$ and $\phi = 0°$. (A) The copper and nitroxyl regions of the experimental spectrum. There is a 37 G overlap of the high-field portion of the 520-G scan of the copper lines and the low-field portion of the 200-G scan of the nitroxyl lines. The spectra were obtained with 5 mW power and modulation amplitudes of 2 and 1.6 G for the copper and nitroxyl lines, respectively. The gain used to record the copper lines was 10 times that used to record the nitroxyl lines. (B) Calculated spectra obtained for the parameters given in Tables I–III. The zero-crossing points for the nitroxyl hyperfine triplets for each of the species are shown schematically below the calculated spectrum.

Figure 14 shows the spectrum of II obtained for $\theta = 117°$ and $\phi = 90°$. At this orientation the copper hyperfine splitting was 107 G and the nitroxyl nitrogen hyperfine splitting was 28 G. The nitroxyl region of the spectrum was a single broad triplet which indicated that the spin–spin splittings for all the species were close to zero at this orientation of the magnetic field. This spectrum was important in defining possible orientations of the interspin vector for the four species. Furthermore, since the observed nitroxyl nitrogen hyperfine splitting was close to the value of A_{zz}, the spectrum required that the nitroxyl z axis for all the species must lie close to this orientation. Figure 15 shows the spectrum of II obtained for $\theta = 135°$ and $\phi = 0°$. At this orientation the copper hyperfine splitting was 145 G and the nitroxyl nitrogen hyperfine splitting was 11 G. The spin–spin splittings for species 2 and 3 were small at this orientation so the nitroxyl signals were approximately three line patterns which were well-separated from the signals of 1 and 4 for which the spin–spin splitting was larger at this orientation.

The values of r for cis isomer II ranged from 9.2 to 12.5 Å (Table II). The values of ϵ and η have an ambiguity which arises from the inversion symmetry of the Hamiltonian: x, y, z is indistinguishable from $-x, -y, -z$. The values of η were chosen to fall between $\pm 90°$. Thus the orientation of the interspin vector for species 4 was given as $\eta = 80$, $\epsilon = 155$ (Table II). This is symmetry equivalent to $\eta = -100$, $\epsilon = 25$. If the orientation definitions for which ϵ is less than 90 are used for species 1–4, there is a correlation between the values of r and ϵ with larger values of r occurring for larger values of ϵ. This parallels the trend observed for trans isomer I. The values of J range from −4 to $+10 \times 10^{-4}$ cm^{-1}. Thus the values of J for cis isomer II are strongly dependent on the conformation of the spin–label linkage as was found for trans isomer I. For both trans isomer I and cis isomer II, the orientation parameters and the values of r are consistent with strain-free conformations of the molecule obtained with CPK molecular models.

Several interesting aspects of the exchange interaction emerge from a comparison of the values of J obtained for the two isomers. The observation that J can be both positive and negative for closely related conformations of a molecule provides considerable insight into solution studies. For one spin-labeled copper complex it was observed that the value of J in a mixture of solvents was smaller than the value of J observed in either of the solvents alone.[22] On the basis of the present results it is plausible that the sign of J was different in the two solvents. Thus, in looking for trends in the values of J from solution studies it will be necessary to keep in mind that some apparent anomalies may be due to changes in the sign of J. In fluid solution the analysis of AB splitting patterns does not give the sign of J. Kokorin and co-workers have analyzed the temperature dependence of J for a nitroxide biradical and concluded that two conformations of the molecule with different signs of J were rapidly interconverting in solution.[23]

For the major species observed for trans isomer I, the values of J ranged from −12 to -30×10^{-4} cm^{-1}. A minor component was observed with a J of 1×10^{-4} cm^{-1}, but its small population (4%) suggests that it represents an unfavorable conformation of the molecule. For cis isomer I, the values of J ranged from −4 to 10×10^{-4} cm^{-1}. Thus the magnitudes of the values of J observed for the cis isomer are smaller than for the trans isomer. This trend parallels results obtained in fluid solution.[3,6] It is also interesting that the sign of J appears to be consistently negative for the trans isomer, but is either positive or negative for the cis isomer. In proton NMR it has been found that the three-bond coupling constants for protons on olefins are consistently greater for the trans isomer than for the cis isomer, with the sign of J positive for the trans isomer and either positive or negative for the cis isomer.[24,25] In comparing the signs of J from NMR and this EPR study it must be noted that the exchange term in NMR is routinely given as $J S_1 \cdot S_2$, whereas in this paper we have used $-J S_1 \cdot S_2$.

(22) DuBois, D. L.; Eaton, G. R.; Eaton, S. S. *J. Am. Chem. Soc.* **1978**, *100*, 2686–2689.
(23) Kokorin, A. I.; Shubin, A. A.; Parmon, V. N. *Izv. Akad. Nauk. SSSR, Ser. Khim.* **1981**, 2023–2028 (1660–1663 in transl.).
(24) Emsley, J. W.; Feeney, J.; Sutcliffe, L. H. "High Resolution NMR Spectroscopy", Vol. 2, p 727 ff.
(25) Sternhell, S. *Q. Rev. Chem. Soc.* **1969**, *23*, 236–270.

Therefore the sign conventions are opposite. In fluorine NMR the three-bond coupling constants for fluorines attached to olefins are consistently greater for the trans isomer than for cis isomer, and where sign information has been obtained, the sign of J for the trans isomer is negative but the sign of J for the cis isomer is positive.[26] Thus for fluorine coupling constants the signs of J for the cis and trans isomers are opposite and reversed from the signs of the EPR coupling constants reported here. For a variety of other nuclei it has also been observed that for 3- and 4-bond couplings across an olefinic linkage, the coupling constant is greater for the trans isomer than for the cis isomer.[27-30] Since the EPR couplings are through 10 bonds, there are undoubtedly many other factors that influence the magnitude of J than just the conformation of the olefin; however, it appears that the effect of the olefinic linkage on the magnitude of the EPR coupling constants parallels the effect of the same linkage on NMR couplings.

It has been stated that the value of J decreases exponentially with increasing values of r.[31,32] An exponential dependence of exchange on r is also assumed in fluorescence energy transfer studies.[33] However, for the conformations of I and II observed in ZnTPP there is no correlation between the values of r and J. Thus, although there may be a dependence of J on r for direct overlap of the orbitals containing the unpaired electrons, there is no such relationship when the interaction is through a series of intervening orbitals as in I and II. It has also been reported that in titanium dimers with organic bridging ligands there was no correlation between the values of J and r.[34]

The EPR spectrum of I has also been examined in a frozen solution of toluene and THF.[5] Simulation of the spectra gave r = 13.5 Å, $\epsilon = 75°$, and $J = -40 \times 10^{-4}$ cm^{-1}.[5] The g and A values for the copper and nitroxyl electrons in the frozen solution were in good agreement with the values reported in Tables I and III. Other conformations may have been present in the frozen solution, but their presence was not detected. The values of r and J obtained from the frozen spectrum are different from the values obtained for any of the species in the ZnTPP single crystal. A powder sample of I in ZnTPP gave a poorly resolved spectrum, but the extent of the nitroxyl region of the spectrum clearly indicated that no conformation of I was present in which the spin-spin splitting of the nitroxyl lines was as large as that observed in the frozen solution spectrum in toluene-THF. Therefore it was concluded that the differences in the parameters obtained in the single crystal and in frozen solution were due to differences in the conformation of I in the two environments and not to difficulties in the analysis of the spectra. The differences in conformations in the two environments suggest that crystal packing forces in the host lattice may have a substantial impact on the detailed conformation of the spin-labeled linkage in these copper complexes.

Conclusions

Analysis of the single-crystal EPR spectra of spin-labeled copper complexes I and II doped into ZnTPP has given a detailed picture of the exchange and dipolar contributions to the spin-spin interaction. Four conformations of each isomer were observed. The magnitude of the exchange coupling constant, J, was strongly dependent on the conformation of the molecule and was larger for trans isomer I than for cis isomer II. The sign of J was positive for some conformations and negative for other conformations. There was no correlation between the value of J and the interspin distance, r.

There is an increasingly strong analogy between NMR nuclear coupling constants and EPR electron-electron coupling constants. It has been known for some time that the signs and magnitudes of NMR coupling constants are dependent on molecule conformation, but this study provides the clearest evidence to date that EPR coupling constants have a similar dependence. It is anticipated that further studies of EPR electron-electron coupling constants will become as important an aspect of EPR spectroscopy as nuclear coupling constants are in NMR.

Acknowledgment. This work was supported in part by NIH Grant GM21156.

Registry No. I, 76451-29-1; II, 76497-30-8; ZnTPP, 14074-80-7.

(26) Emsley, J. W.; Phillips, L.; Wray, V. *Prog. NMR Spectrosc.* **1978**, *10*, 83-756.
(27) Voegeli, U.; Philipsborn, W. *Org. Magn. Reson.* **1975**, *7*, 617-627.
(28) Prokofev, E. P.; Karpeiskaya, E. I. *Tetrahedron. Lett.* **1979**, 737-740.
(29) Ten Hoedt, R. W. M.; Van Koten, G.; Noltes, J. *G. J. Organomet. Chem.* **1979**, *170*, 131-149.
(30) Estaigh-Hosseini, H.; Kroto, H. W.; Nixon, J. F.; Brownstein, S.; Morton, J. R.; Preston, K. F. *J. Chem. Soc., Chem. Commun.* **1979**, 653-654.
(31) Coffman, R. E.; Buettner, G. R. *J. Phys. Chem.* **1979**, *83*, 2392-2400.
(32) McNally, J. M.; Kreilick, R. W. *Chem. Phys. Lett.* **1981**, *79*, 534-540.
(33) Stryer, L.; Thomas, D. D.; Meares, C. F. *Ann. Rev. Biophys. Bioeng.* **1982**, *11*, 203-222.
(34) Francesconi, L. C.; Corbin, D. R.; Clauss, A. W.; Hendrickson, D. N.; Stucky, G. D. *Inorg. Chem.* **1981**, *20*, 2059-2069.

Intermolecular Motional Degrees of Freedom of H_2O and D_2O Isolated in Solid Gas Matrices

Erich Knözinger* and Rüdiger Wittenbeck

Contribution from the Institut für Physikalische Chemie, Universität Siegen, D-5900 Siegen 21, Federal Republic of Germany. *Received August 4, 1982*

Abstract: Disordered solids of pure noble gases (Ar, Kr, Xe) as well as these matrices doped with H_2O and D_2O (1:1000) were studied by far-IR Fourier spectroscopy at very low temperatures (10 K). Previous neutron diffraction studies and the temperature dependence of the far-IR spectra measured in this study permit assignment of the IR-active phonon absorption of pure solid inert gas matrices. There is conclusive evidence that water introduced in these matrices at very low concentrations (1:1000) is present in the form of two fundamentally different species: (1) nearly freely rotating water molecules that have IR-active rotational transitions below 40 cm^{-1}, and (2) inert gas hydrates that contribute IR-active intermolecular vibrations between 40 and 100 cm^{-1}. In solid nitrogen the relevant spectral range is free of characteristic H_2O absorption, indicating that free rotation does not occur. The interaction between N_2 and H_2O gives rise to intermolecular vibrations located considerably above 100 cm^{-1}.

Far-infrared spectroscopic observations of polar and nonpolar molecules embedded in solid inert gas matrices promise to provide an extremely important tool for the study of intermolecular interactions. Experimental determination of the concentration and temperature dependence of the low-frequency bands enables intermolecular vibrations of aggregates to be distinguished from vibrations of the isolated monomer molecules relative to the cage. In addition, the character of the motion may be described

0002-7863/83/1505-2154$01.50/0